**The EMBO Journal (2011) 30,** 665–678 | © 2011 European Molecular Biology Organization | All Rights Reserved 0261-4189/11
www.embojournal.org

THE EMBO JOURNAL

# Cdc42-dependent formation of the ZO-1/MRCKβ complex at the leading edge controls cell migration

**Lin Huo[1], Wenyu Wen[1,2,3], Rui Wang[1], Chuen Kam[1], Jun Xia[1], Wei Feng[1,4,*] and Mingjie Zhang[1,*]**

[1]Division of Life Science, Molecular Neuroscience Center, State Key Laboratory of Molecular Neuroscience, Hong Kong University of Science and Technology, Clear Water Bay, Kowloon, Hong Kong, [2]Department of Chemistry, Shanghai, China, [3]Institutes of Biomedical Sciences, Fudan University, Shanghai, China and [4]National Laboratory of Biomacromolecules, Institute of Biophysics, Chinese Academy of Sciences, Beijing, China

**Zonula occludens (ZO)-1 is a multi-domain scaffold protein known to have critical roles in the establishment of cell–cell adhesions and the maintenance of stable tissue structures through the targeting, anchoring, and clustering of transmembrane adhesion molecules and cytoskeletal proteins. Here, we report that ZO-1 directly binds to MRCKβ, a Cdc42 effector kinase that modulates cell protrusion and migration, at the leading edge of migrating cells. Structural studies reveal that the binding of a β hairpin from GRINL1A converts ZO-1 ZU5 into a complete ZU5-fold. A similar interaction mode is likely to occur between ZO-1 ZU5 and MRCKβ. The interaction between ZO-1 and MRCKβ requires the kinase to be primed by Cdc42 due to the closed conformation of the kinase. Formation of the ZO-1/MRCKβ complex enriches the kinase at the lamellae of migrating cells. Disruption of the ZO-1/MRCKβ complex inhibits MRCKβ-mediated cell migration. These results demonstrate that ZO-1, a classical scaffold protein with accepted roles in maintaining cell–cell adhesions in stable tissues, also has an active role in cell migration during processes such as tissue development and remodelling.**

*The EMBO Journal* (2011) **30,** 665–678. doi:10.1038/emboj.2010.353; Published online 14 January 2011
*Subject Categories*: cell & tissue architecture; structural biology
*Keywords*: cell migration; MRCKβ; scaffold protein; ZO-1; ZU5 domain

## Introduction

Tight junctions (TJs), localized to the apical ends of the basolateral domains of plasma membranes, have key roles in regulating paracellular permeability and maintaining the apico-basal polarity of epithelial cells (Balda and Matter, 1998; Matter and Balda, 2003; Anderson *et al*, 2004). In addition to their prime function as barriers and fences, TJs also contain proteins involved in the regulation of numerous cellular functions. To date, >40 different TJ proteins have been discovered (D'Atri and Citi, 2002; Gonzalez-Mariscal *et al*, 2003; Schneeberger and Lynch, 2004). They can be divided into two groups. The first group are the integral membrane TJ proteins, including occludins, claudins, and JAMs (junctional adhesion molecules), which bridge apical intercellular spaces and form physical barriers (Furuse *et al*, 1993, 1998; Martin-Padura *et al*, 1998). The second group are the plaque proteins (e.g. zonula occludens (ZO)-1, ZO-2, ZO-3, cingulin, MAGI, Crumbs/PALS/PATJ, Par-3/Par-6/aPKC complex, etc), which serve as scaffolds to assemble integral membrane proteins, actin cytoskeletons, and cytosolic proteins in TJs (Citi *et al*, 1988; Ide *et al*, 1999; Gonzalez-Mariscal *et al*, 2000; Roh *et al*, 2002; Hurd *et al*, 2003). Extensive studies have generated a wealth of information pertaining to the functions of these proteins in the formation of cell–cell junctions, but the functions of these junctional proteins during tissue development and remodelling (i.e. before the formation of stable cell–cell junctions) are much less clear.

ZO-1 was the first TJ protein identified (Stevenson *et al*, 1986). Together with ZO-2 (Jesaitis and Goodenough, 1994) and ZO-3 (Haskins *et al*, 1998) they all belong to the membrane-associated guanylate kinase (MAGUK) family of scaffold proteins, and these three proteins are now collectively called TJ MAGUKs (Woods and Bryant, 1993; Anderson *et al*, 1995; Kim, 1995). Each of these three ZO proteins contains three PDZ (*P*SD-95/*D*iscs large/*Z*O-1) domains, one SH3 (Src-homology 3) domain, and one GK (guanylate kinase) domain (Figure 1A) (Itoh *et al*, 1993; Willott *et al*, 1993; Jesaitis and Goodenough, 1994; Haskins *et al*, 1998). In contrast to other MAGUK proteins, ZO proteins (ZO-1 and ZO-2 in particular) contain a long proline-rich carboxyl terminal region that may be responsible for their unique properties in TJs (Jesaitis and Goodenough, 1994; Itoh *et al*, 1997; Fanning *et al*, 1998; Gonzalez-Mariscal *et al*, 1999; Ryeom *et al*, 2000). Interestingly, ZO-1 also contains an additional ZU5 domain (initially found in *Z*O-1 and *UNC5*; Ackerman *et al*, 1997; Leonardo *et al*, 1997) at its C-terminus (Figure 1A). ZO proteins have long been assumed to have essential roles in TJ establishment and epithelial polarity maintenance, as their PDZ domains directly bind to the carboxyl tails of claudins and their GK domains interact with occludins (Fanning *et al*, 1998; Haskins *et al*, 1998; Itoh *et al*, 1999). Indeed, the simultaneous deletion of ZO-1 and ZO-2 leads to the complete disappearance of TJs in epithelial cell cultures, indicating that ZO-1 and ZO-2 are required for the formation of TJs (Umeda *et al*, 2006).

*Corresponding authors. W Feng or M Zhang, Division of Life Science, Molecular Neuroscience Center, State Key Laboratory of Molecular Neuroscience, Hong Kong University of Science and Technology, Clear Water Bay, Kowloon, Hong Kong. Tel.: +86 10 6488 8751; Fax: +86 10 6488 8237; E-mail: wfeng@ibp.ac.cn or Tel.: +852 2358 8709; Fax: +852 2358 1552; E-mail: mzhang@ust.hk

**Received: 10 September 2010; accepted: 17 December 2010; published online: 14 January 2011**

Although both mutations are embryonically lethal, mice lacking *ZO-1* and *ZO-2* display distinct phenotypes, indicating that the two scaffold proteins have non-redundant roles in animal development (Katsuno *et al*, 2008; Xu *et al*, 2008). *ZO-2*$^{-/-}$ mice died shortly after implantation because of an arrest in early gastrulation with decreased proliferation at E6.5 (Xu *et al*, 2008). In contrast, *ZO-1*$^{-/-}$ mice embryos are indistinguishable from *ZO-1*$^{+/+}$ mice at E9.5 or earlier, and embryonic development defects of *ZO-1*$^{-/-}$ mice begin appearing at E10.5 (Katsuno *et al*, 2008). Interestingly, *ZO-1*$^{-/-}$ mice embryos also display severely inhibited angiogenesis in their yolk sacs without defects in vasculogenesis. In view of

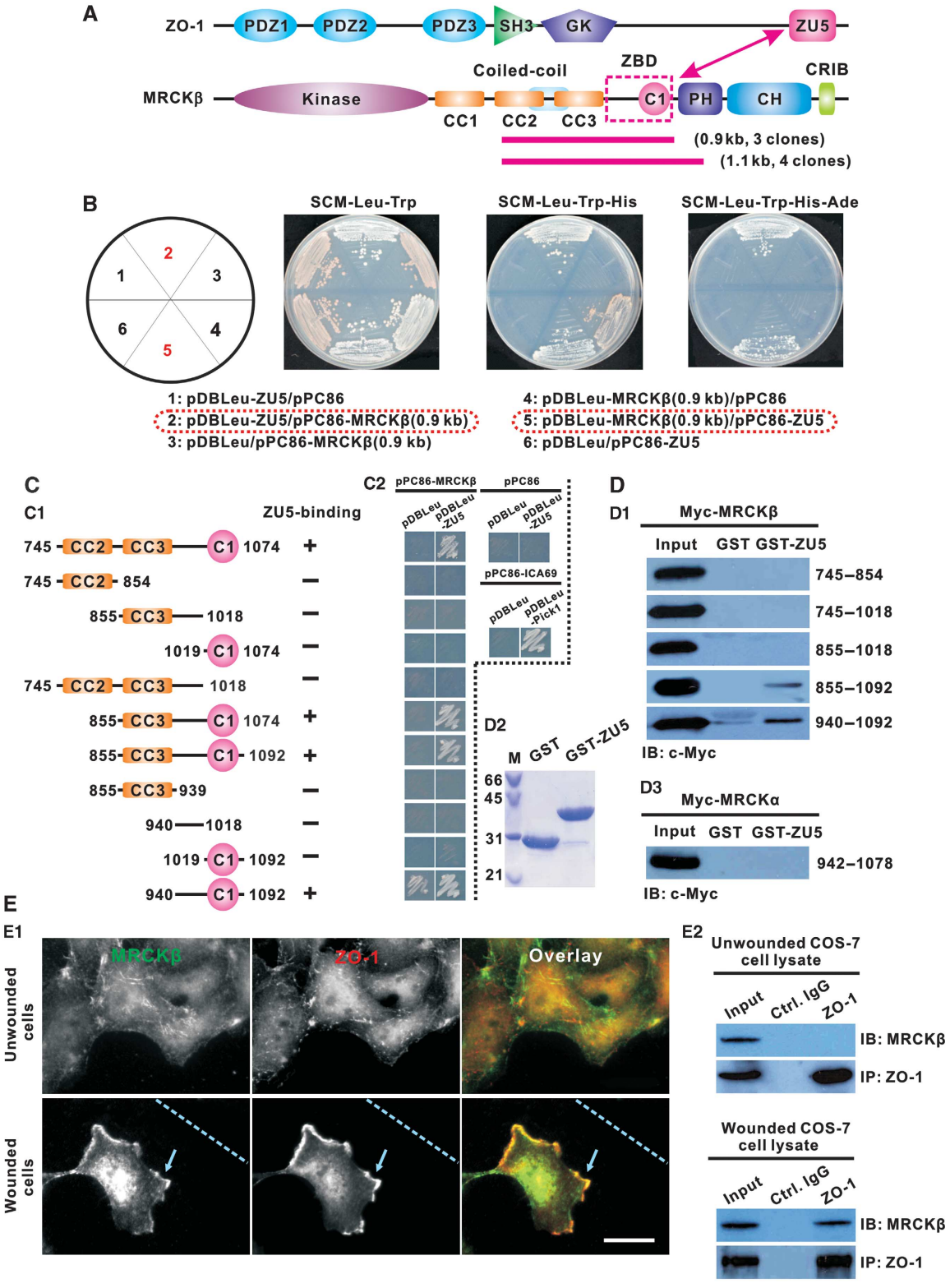

the well-accepted roles of ZO-1 in the formation of TJs, this inhibited angiogenesis is thought to be the result of defects in cell–cell adhesions (Katsuno *et al*, 2008). An alternative explanation is that it is caused by vessel endothelial cell migration defects. It has recently been shown that α5-integrin and ZO-1 physically interact with each other at the leading edge of migrating cells (Tuomi *et al*, 2009), suggesting that ZO-1 has a role in cell migration in addition to its well-accepted roles in mediating cell adhesion. Consistent with the observed α5-integrin and ZO-1 interaction, α5-integrin null mice share a number of phenotypes with *ZO-1*$^{-/-}$ mice (Goh *et al*, 1997). In cell culture models, ZO-1 and ZO-2 can partially replace each other both in TJ formation and in polarity establishment in cultured epithelia. However, ZO-1$^{-/-}$ cells need a significantly longer time to form TJs and to polarize fully in spite of the upregulated expression of ZO-2 (Umeda *et al*, 2006), implying that the C-terminal ZU5 domain of ZO-1 is important for the establishment of cell polarity and possibly cell migration (ZO-2 lacks a ZU5 domain). It has been shown that the deletion of the ZU5 domain leads to a partial dissociation of ZO-1 from TJs to the cytoplasm in MDCK cells (McNeil *et al*, 2006), although the underlying molecular mechanism is unclear.

Here, we show that ZO-1 physically interacts with MRCKβ, a Cdc42 effector kinase involved in the membrane protrusions of motile cells (Leung *et al*, 1998; Gomes *et al*, 2005; Wilkinson *et al*, 2005; Tan *et al*, 2008), via its ZU5 domain. The biochemical basis of the ZO-1 ZU5 domain-mediated MRCKβ interaction is characterized in detail. We further show that a fraction of ZO-1 specifically localizes at and targets MRCKβ to the leading edge of migrating cells. We discover that the formation of the ZO-1/MRCKβ complex requires the binding of Cdc42 to the kinase. Finally, we demonstrate that the ZO-1-mediated positioning of MRCKβ at the leading edge of cells is necessary for their migrations. Our studies reveal that, in addition to its well-accepted roles in mediating cell–cell adhesion of organized tissues, ZO-1 also has an active role in cell migrations, and thus is likely to be linked to diverse cellular processes ranging from tissue remodelling in the development to cancer cell migrations.

## Results

### *ZO-1 binds to MRCKβ via its unique ZU5 domain*

We hypothesized that the unique ZU5 domain of ZO-1 is at least partly responsible for the differences between the functions of ZO-1 and ZO-2. To test this hypothesis, we searched for potential ZO-1 ZU5-binding proteins using yeast two-hybrid screening (Y2H) with the wild-type (WT) ZU5 domain as the bait. Among 10 positive clones isolated under the highly stringent screening condition, seven encode partial fragments of MRCKβ sharing an overlapping region consisting of 330 amino-acid residues (residues 745–1074; Figure 1A and B). Y2H-based assays and *in vitro* biochemical binding experiments were further used to map out the minimal ZO-1 ZU5-binding fragment of MRCKβ (Figure 1C and D), which consists of a 153-residue fragment (referred to as ZBD for *Z*O-1-*b*inding *d*omain), including the C1 domain and a connecting sequence between the CC3 (the coiled-coil three region) and the C1 domain of MRCKβ (Figure 1A, C, and D). Interestingly, neither Y2H nor *in vitro* binding assays could detect any interaction between ZO-1 ZU5 and MRCKα (Figure 1D3), indicating that ZO-1 ZU5 specifically binds to the β isoform of MRCK (see Figure 5 for more details).

To our surprise, the endogenous ZO-1 and MRCKβ do not seem to interact with each other in COS-7 cells cultured to near confluent states, as MRCKβ is largely diffused in cytosol and nuclei with enrichment in cell periphery (cell protrusions in particular) (Leung *et al*, 1998), whereas ZO-1 is diffused throughout the cells (Figure 1E1, top panels). Scratch wounding of COS-7 cells led to drastic changes in the localizations of both ZO-1 and MRCKβ in cells facing the wounding front. In these wounded cells, a large portion of ZO-1 becomes to localize at the leading edge of the wounded cells (Figure 1E1; Supplementary Figure S1A). Concomitantly, a significant proportion of MRCKβ is also localized at the leading edge of the wounded cells together with ZO-1 (Figure 1E1). A co-immunoprecipitation assay showed that endogenous ZO-1 and MRCKβ physically associate with each other only in wounded COS-7 cells (Figure 1E2). The above results indicate that the interaction between ZO-1 and MRCKβ only occurs in motile cells (see Figure 6 for more details). We further showed that the leading edge co-localization of ZO-1 and MRCKβ was also detected in two migrating human cancer cell lines (Supplementary Figure S2), pointing to a potential general role of the ZO-1/MRCKβ complex in cell migrations.

### *ZO-1 anchors MRCKβ at the leading edge of migrating cells*

We next asked whether ZO-1 determines MRCKβ localization at the leading edge of migration cells or *vice versa* by transiently transfecting COS-7 cells with RFP-tagged MRCKβ and GFP-tagged ZO-1. Co-transfection of the WT MRCKβ and ZO-1 led to prominent co-localization of the two proteins at the leading edge of transfected cells (Figure 2A3 and D). Deletion of ZBD from MRCKβ dramatically reduced its lead-

**Figure 1** ZO-1 specifically binds to MRCKβ via its ZU5 domain. (**A**) Domain organization of ZO-1 and MRCKβ. ZO-1 contains three N-terminal PDZ domains followed by a SH3-GK tandem, and a unique C-terminal ZU5 domain. MRCKβ is composed of, in order from its N- to C-termini: a kinase domain, three coiled-coil domains, and C1-PH-CH-CRIB domains arranged in tandem. The two magenta lines underneath MRCKβ represent the seven overlapping clones identified in the Y2H screening using ZO-1 ZU5 as the bait. (**B**) Y2H assays showing the strong and specific interaction between an ~0.9 kb MRCKβ fragment encoding amino-acid residues 745–1074 and the ZO-1 ZU5 domain. (**C**, **D**) Mapping of the minimal ZO-1 ZU5-binding region of MRCKβ (residues 940–1092) by a Y2H-based binding assay (**C**) and an *in vitro* GST pull-down assay (**D**). The corresponding region in MRCKα failed to bind to ZO-1 ZU5, showing the specificity of the interaction between ZO-1 and MRCKβ. The weak growth of the 940–1092 construct (bottom right panel of C2) presumably is due to self-activation of the fragment in the Y2H assay. (**E**) ZO-1 specifically interacts with MRCKβ in motile cells. ZO-1 and MRCKβ show specific co-localization at the leading edge of migrating cells (E1, lower panel). In contrast, no obvious co-localization between ZO-1 and MRCKβ could be observed when cells were cultured to near confluence (E1, upper panel). In this assay, directed cell migration was induced by scratching confluent cells with a pipette indicated by the dashed lines at the bottom panels of (E1). The leading edge of the wounded cells was identified by rhodamine-conjugated phalloidin staining of actins (Supplementary Figure S1A). Scale bar: 10 μm. Endogenous MRCKβ was co-immunoprecipitated by endogenous ZO-1 in wounded COS-7 cell lysates using an anti-ZO-1 antibody (E2). No detectable ZO-1/MRCKβ interaction was found in unwounded cells.

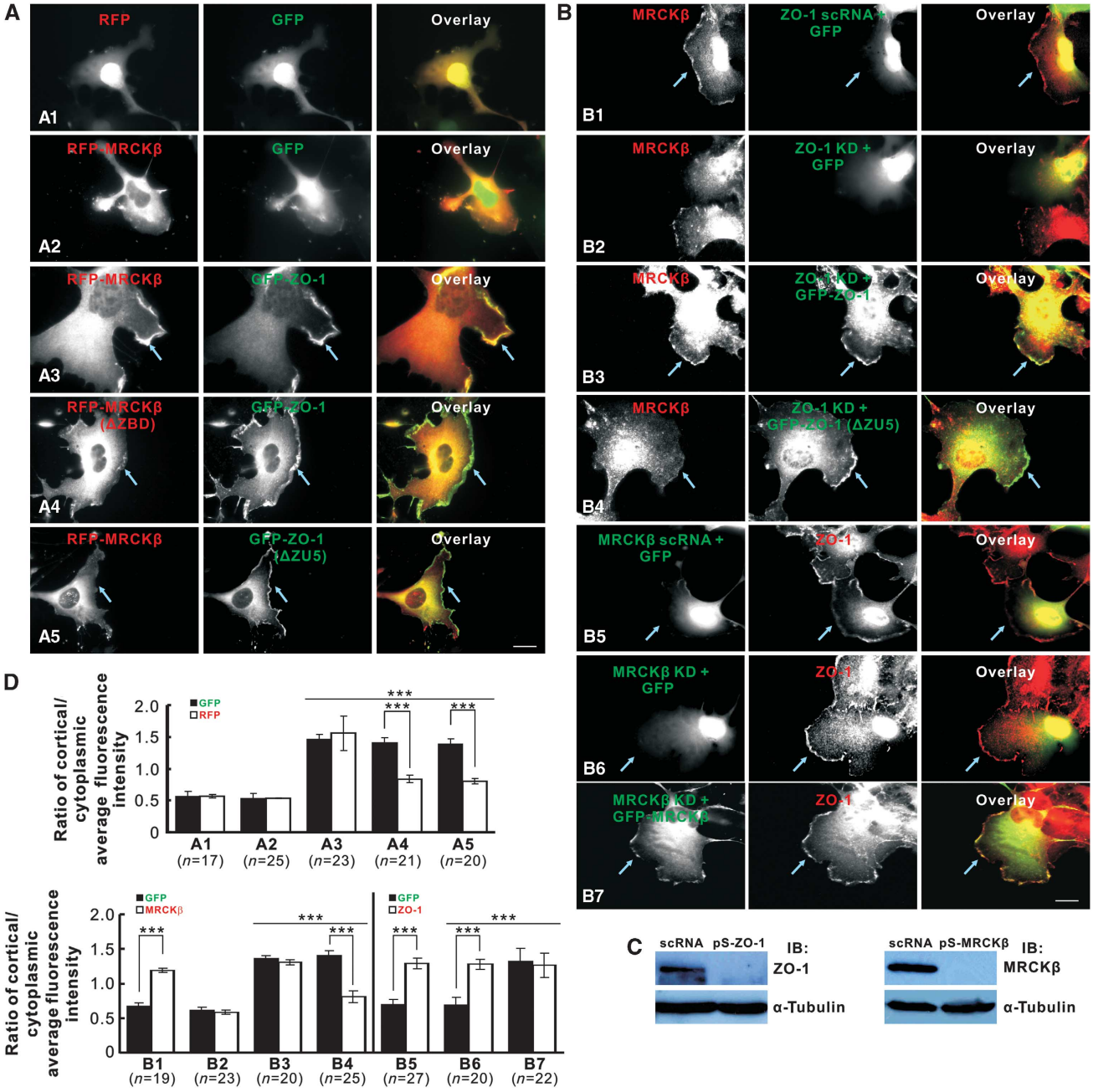


**Figure 2** ZO-1 anchors MRCKβ at the leading edge of migrating cells. (**A**) When overexpressed, a fraction of ZO-1 and MRCKβ are co-localized at the leading edge of migrating COS-7 cells (A3). RFP and GFP served as the controls and show diffused distribution throughout the cytoplasm and nucleus (A1), and GFP alone cannot target RFP-MRCKβ to the leading edge (A2). Deletion of the ZO-1-binding domain (ZBD) from MRCKβ (A4) or removal of the ZU5 domain from ZO-1 (A5) severely impaired the leading edge localization of MRCKβ but not ZO-1. (**B**, **C**) The leading edge localization of MRCKβ was not affected by the scramble siRNA (scRNA) of ZO-1 (B1). Knockdown of ZO-1 disrupted the leading edge localization of MRCKβ (B2), which could be rescued by the RNAi-resistant WT ZO-1 (B3) but not by ZO-1 with its ZU5 domain removed (B4). Both the scRNA of MRCKβ and knockdown of MRCKβ had no effect on endogenous ZO-1 leading edge localization (B5, B6), and the RNAi-resistant WT MRCKβ was found to co-localize with ZO-1 at the leading edge (B7). The knockdown efficiencies of shRNAs were evaluated by western blot analysis (**C**). Scale bar: 20 μm. (**D**) Quantification of leading edge localizations of ZO-1 and MRCKβ in experiments is shown in (**A**, **B**). The ratio of average fluorescence intensities of membrane cortex over cytoplasm was used to measure leading edge enrichments of ZO-1 and MRCKβ in each cell. Error bars represent SEM. '*n*' represents the number of cells analysed in each experiment. ***$P<0.0005$ by the Student's *t*-test.

ing edge localization, but the leading edge localization pattern of ZO-1 did not change (Figure 2A4 and D). Conversely, although the deletion of the ZU5 domain did not change the leading edge localization of ZO-1, essentially no MRCKβ was found at the leading edge of the co-transfected cells (Figure 2A5 and D). Thus, the binding of ZO-1 through its ZU5 domain to MRCKβ ZBD serves to target the enzyme to the leading edge of migrating cells, and regions outside of the ZU5 domain in ZO-1 determine its own leading edge localization in migrating cells. The PDZ domains of ZO-1 might be

 

responsible for its leading edge localization by binding to α5-integrin (Tuomi *et al*, 2009).

To avoid possible interference from endogenous proteins in the transient transfection experiments, we removed them individually via the RNAi approach and repeated the above experiments. Knockdown of ZO-1 eliminated the leading edge localization of the endogenous MRCKβ but not MRCKα (Figure 2B2, C, and D; Supplementary Figure S1B), indicating that ZO-1 is specifically required for the leading edge localization of MRCKβ. As expected, transfection of the RNAi-resistant WT ZO-1 rescued the leading edge localization of MRCKβ, but the ZO-1 mutant without its ZU5 domain did not rescue the WT ZO-1 knockdown even though the mutant itself was well localized to the leading edge (Figure 2B3, B4, and D). Consistent with the results from the overexpression experiments, knockdown of MRCKβ did not change the leading edge localization of ZO-1 (Figure 2B6, C, and D). The RNAi-resistant MRCKβ expressed was also found to co-localize with the endogenous ZO-1 at the leading edge of the transfected cells (Figure 2B7 and D). Taken together, the above data reveal that ZO-1 acts upstream of MRCKβ in anchoring the ZO-1/MRCKβ complex at the leading front of migrating cells.

### *ZO-1 ZU5 adopts a partial ZU5-fold*

To elucidate the mechanistic basis of ZO-1 ZU5-mediated MRCKβ binding, we tried to determine the three-dimensional structure of the domain using NMR spectroscopy. Due to poor sample behaviour caused by unfavourable conformational exchanges and non-specific aggregations (Supplementary Figure S3, and see below), the WT ZO-1 ZU5 (residues 1631–1748) is not amendable for NMR-based structure determination. Aided by extensive amino-acid sequence analysis and structural predictions, we tested numerous point as well as deletion mutations (>30) of the domain by inspecting the $^{1}H$–$^{15}N$ HSQC spectrum of each mutant. One of such mutants, with Met1699 and Cys1700 substituted with Ala (referred to as ZU5_MC/AA) displayed an excellent sample condition suitable for NMR-based structure determination of the domain (Supplementary Figure S3A).

The solution structure of ZU5_MC/AA was determined to a high resolution using NMR spectroscopy (Figure 3; Supplementary Table 1). Except for two loops (the β4/β5 and β7/β8 loops) that are intrinsically flexible (Figure 3A; Supplementary Figure S3C), all the other regions of the domain are well defined. The ZU5 domain adopts a β-barrel fold formed by two anti-parallel β sheets packed with each other in parallel. The first β sheet contains four strands (β1, β4–6), and the second one contains another four strands (β2, 3, 7, and 8) (Figure 3B). A comparison of the HSQC spectrum of the WT ZU5 domain at low concentration (i.e. not heavily aggregated form) with that of the MC/AA mutant revealed that most of the peaks from the WT ZU5 overlapped well with or only experienced relatively small shifts with respect to those from the MC/AA mutant; the exceptions are the residues from β5, β6, and part of β4, indicating that the overall conformation of the protein is not altered by the mutation (Supplementary Figure S3A and B). The residues of the WT ZU5 domain that experience significant mutation-induced shift changes display either doublets or very broad peaks in the HSQC spectrum (Supplementary Figure S3A and B), indicating that these residues (β5 and the β4/β5 loop in particular) undergo slow-to-intermediate conformational exchanges. The most likely interpretation of these data is that the WT ZO-1 ZU5 adopts two distinct conformations: one seen in the structure of the MC/AA mutant with β5 pairing with β6, and the other with β5 swinging out to form an ill-defined loop connecting β4 and β6 (Supplementary Figure S3D). The structure seen in the MC/AA mutant represents the closed conformation, as the mutant cannot bind to MRCKβ (Figure 4A1 and B). The conformation with β5 not paired with β6 represents an open state capable of binding to MRCKβ (Supplementary Figure S3D and see below for details).

Next, we explored the structural requirements on ZO-1 ZU5 for its binding to MRCKβ. The residues forming the β8 strand ('VSVLI') at the extreme C-terminal end of ZO-1, which is predicted not to be a part of ZU5 domain, make extensive hydrophobic contact with the rest of the ZU5 domain (Figure 3D). All the residues involved in the hydrophobic interactions are evolutionarily conserved (Figure 3E). Additionally, the bulky aromatic ring of the last residue Phe1748 of ZO-1 is inserted into a hydrophobic pocket (Figure 3D), further stabilizing the interaction between the ZU5 domain and the C-terminal tail. Deletion of the entire C-terminal fragment or even only Phe1748 both lead to the complete disruption of the interaction between ZO-1 and MRCKβ, assayed through *in vitro* biochemical binding experiments and using an imaging-based assay for the ZO-1-mediated leading edge localization of MRCKβ (Figure 4A2, A3, C2, C3, and D). As a control, the addition of an Ala residue to the C-terminus of ZO-1 has no effect on the ZO-1-mediated localization of MRCKβ (Figure 4A4 and C4). Thus, the structural integrity of the ZU5 domain is required for ZO-1 to interact with MRCKβ.

We note that the 3D structure of ZO-1 ZU5 is significantly different from the recently determined structures of the ZU5 domains from Unc5H2 (Wang *et al*, 2009) and ankyrin-R (Ipsaro *et al*, 2009). The β barrel of ZO-1 ZU5 contains 8 β strands, compared with 12 in UNC5 ZU5 and 11 in ankyrin-R ZU5 (Supplementary Figure S4). Amino-acid sequence alignment analysis, together with the structures of these three ZU5 domains, reveals that ZO-1 ZU5 lacks the sequences corresponding to the β8, β9, β10, and β12 strands of UNC5 ZU5 and the β8, β9, and β11 strands of ankyrin ZU5 (Supplementary Figures S4 and S7), indicating that the ZO-1 ZU5 domain adopts a partial ZU5-fold. Interestingly, the solvent-exposed surface of ZO-1 ZU5 corresponding to the missing β strands side is highly hydrophobic (Figure 3C), and this hydrophobic surface is responsible for the binding between the partial ZU5 domain and MRCKβ (see below for details).

### *Structural basis of the ZO-1/MRCKβ complex formation*

The optimal experiment to elucidate the molecular basis governing the ZO-1 and MRCKβ interaction would be to determine the structure of the ZO-1 ZU5/MRCKβ complex. However, due to the poor behaviour of numerous complex samples, we were not able to achieve this goal either by NMR spectroscopy or by X-ray crystallography. As an alternative approach, we investigated the structural basis of the interaction between the WT ZO-1 ZU5 (not the MC_AA mutant as it does not bind to MRCKβ) and GRINL1A (glutamate receptor, ionotropic, *N*-methyl-D-aspartate-like 1A combined protein;

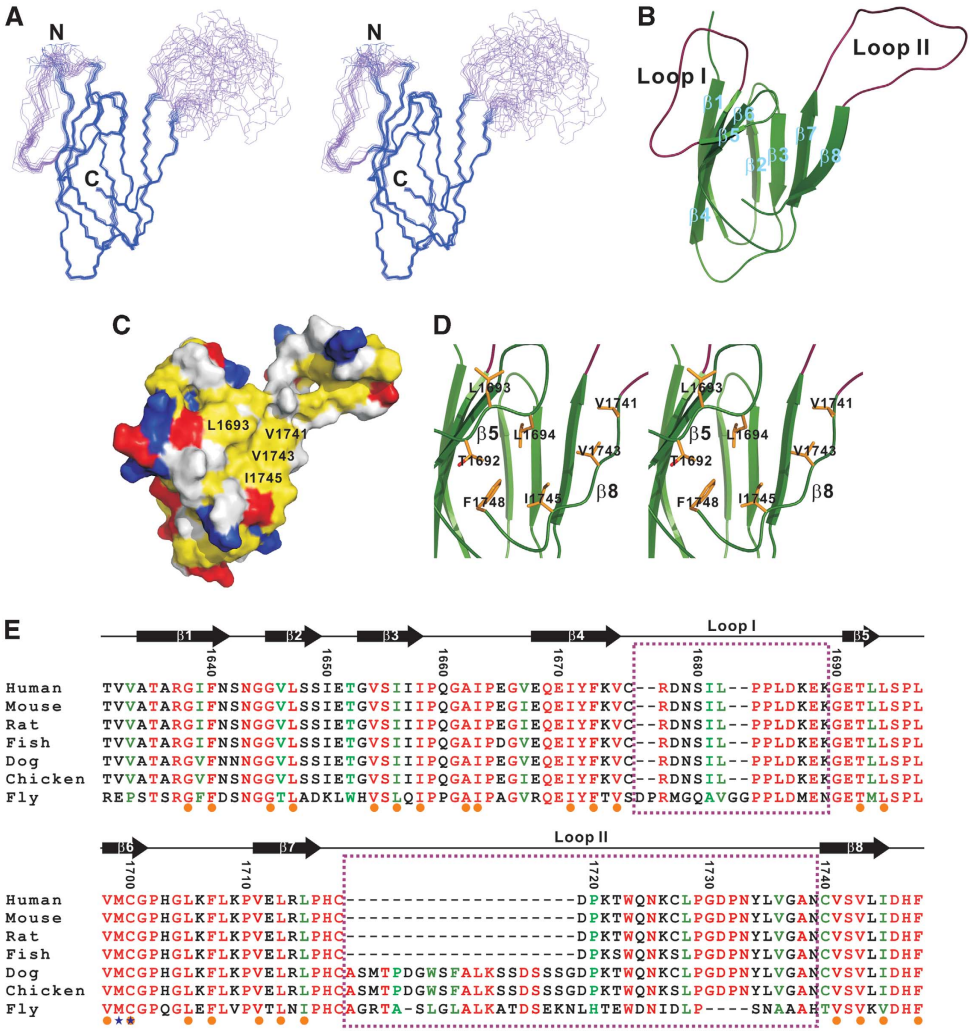


**Figure 3** Solution structure of the ZO-1 ZU5 domain. (**A**) Stereo-view showing the backbones of 20 superimposed NMR-derived structures of ZU5_MC/AA. The two flexible loops are coloured in purple. (**B**) Ribbon diagram of a representative structure of ZU5_MC/AA. The secondary structures (β1–β8) are labelled. The two flexible β4/β5 and β7/β8 loops are labelled with loop I and loop II, respectively. (**C**) Surface representation of ZU5_MC/AA. Positively charged residues are drawn in blue, negatively charged residues in red, hydrophobic residues in yellow, and the rest in grey. The residues from the last β strand, together with the β5 and β6 strands of the domain, form a large solvent-exposed hydrophobic surface that is directly responsible for binding to its targets. (**D**) A stereo-view showing the hydrophobic packing of the last β strand (β8) and the extreme C-terminal Phe (Phe1748) with the β-barrel core of the ZU5 domain. The residues involved in the packing are drawn in the explicit atomic representation. The orientation of the domain is the same as that in (**B**). (**E**) Amino-acid sequence alignment of ZO-1 ZU5 from different species, showing the highly conserved nature of the domain throughout the evolution. In this alignment, the absolutely conserved amino acids are highlighted in red, and the highly conserved residues are in green. The residues forming the hydrophobic core are highlighted by orange dots, and Met1699 and Cys1700, which were substituted with Ala for the structural determination of the apo-ZO-1 ZU5 domain, are indicated by blue stars. The residues forming loops I and II are marked by two dashed boxes in purple.

Roginski *et al*, 2004), another binder identified from our Y2H screening. To probe the structural relevance between the ZO-1 ZU5/GRINL1A complex and the ZO-1 ZU5/MRCKβ complex, we used the same set of ZO-1 ZU5 mutants for the disruption of the ZO-1 ZU5/MRCKβ complex (Figure 4C and D) to test their binding to GRINL1A. Neither 'ZO-1 ZU5-ΔCT' nor 'ZO-1 ZU5-ΔF' was capable of binding to the myc-tagged full-length GRINL1A (Supplementary Figure S5A). Additionally, the full-length GRINL1A was found to target ZO-1 ZU5 to junctional membranes in polarized MDCK cells, but failed to do so to the 'ZO-1 ZU5-ΔCT' and 'ZO-1 ZU5-ΔF' mutants (Supplementary Figure S5B). The above results suggest that GRINL1A and MRCKβ likely bind to the same exposed hydrophobic pocket in ZO-1 ZU5 (see Figure 5 for details). Next, a 22-residue peptide fragment of GRINL1A was mapped as the minimal ZO-1 ZU5-binding region (Supplementary Figure S6), and circular dichroism analysis indicated that this 22-residue peptide binds to ZO-1 ZU5 in a β-strand conformation (Supplementary Figure S6C). Finally, we determined the structure of the WT ZO-1 ZU5 in complex with the GRINL1A peptide using NMR spectroscopy (see Supplementary Table 1 and Supplementary Figures S6–S8 for the details of the complex structure).

All of the ZU5 β strands except for β5 adopt similar conformations upon binding to the GRINL1A peptide (Figure 5A). The GRINL1A peptide forms two additional β strands (β9 and β10 hairpin) that pair in parallel with β5 and part of β6 from ZU5. In apo-ZU5_MC/AA, β5 pairs with β6 to form part of the β sheet, thus preventing the target peptide (β9 specifically) from forming anti-parallel β sheet with β5

 

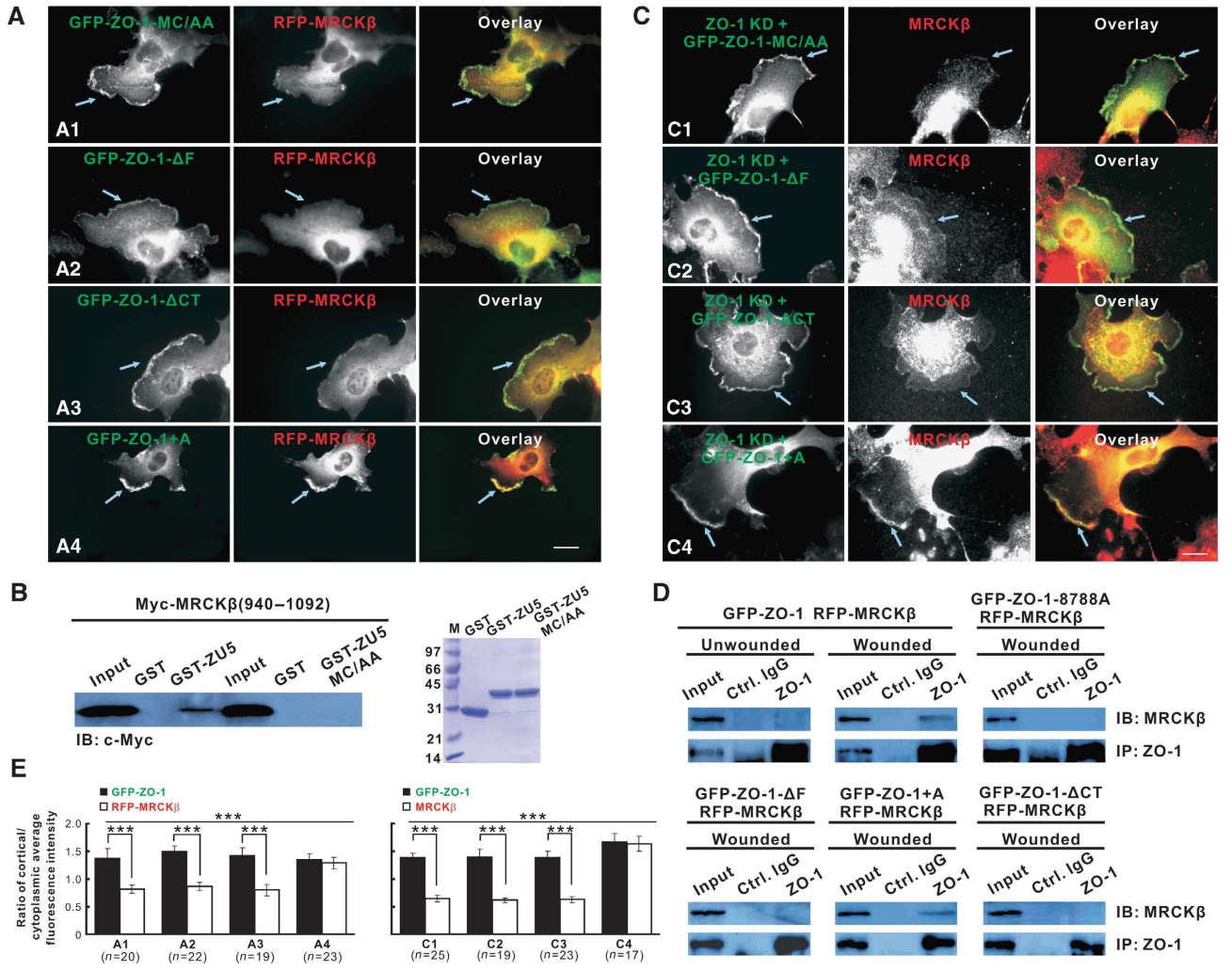


**Figure 4** Conformational requirements of ZO-1 ZU5 for binding to MRCKβ. (**A**) The stabilization of the closed conformation of ZO-1 ZU5 caused by the MC/AA mutation (A1), the deletion of the last Phe (A2), and the removal of the entire β8 (A3) all severely decreased the leading edge localizations of MRCKβ when each of the ZO-1 mutants was co-expressed with MRCKβ in COS-7 cells. As the control, extending ZO-1 at its C-terminal tail by adding an Ala did not have an observable impact on the leading edge localization of MRCKβ (A4). Scale bar: 20 μm. (**B**) GST pull-down assay showing that the MC/AA mutation of ZO-1 ZU5 disrupts its binding to MRCKβ. (**C**) The impairment of the MRCKβ leading edge localization induced by ZO-1 knockdown was not rescued by ZO-1 with the MC/AA mutation (C1), the deletion of Phe1748 (C2), and the deletion of the last β strand (C3), but could be rescued by the ZO-1 mutant with the C-terminal Ala extension (C4). Scale bar: 20 μm. (**D**) Co-IP-based assay showing the interactions between MRCKβ and the various ZO-1 mutants tested in (**A**). In this assay, proteins in each cell lysate were immunoprecipitated with anti-ZO-1 antibody, and co-precipitated proteins were probed with anti-MRCKβ antibody. (**E**) The ratio of average fluorescence intensities of membrane cortex over cytoplasm was used to measure leading edge enrichments of ZO-1 and MRCKβ in each cell. Error bars represent s.e.m. '*n*' represents the number of cells analysed in each experiment. ***$P<0.0005$.

and β6 (i.e. apo-ZU5_MC/AA adopts a closed conformation; see Figure 3 and Supplementary Figure S8A). In the ZU5/GRINL1A peptide complex, β5 dissociates from β6 and swings outwards to one end of the β barrel. Together with β6, it forms a continuous receiving β strand for pairing with β9 of the GRINL1A peptide (Supplementary Figure S8B). The most prominent conformational changes of ZO-1 ZU5 induced by the GRINL1A peptide binding are in the β5 strand (as discussed above) and the β4/β5 loop. While the β4/β5 loop is flexible in apo-ZU5_MC/AA (Figure 3A), it becomes highly ordered in the complex due to its extensive interactions with residues from β5/β6 loop and the β9 strand (Figure 5A; Supplementary Figure S8). The structure of the ZO-1 ZU5/GRINL1A peptide complex, together with the biochemical studies presented in this work, reveals a unique target-binding mechanism. Upon binding to ZO-1 ZU5, the GRINL1A peptide forms a β hairpin that augments the existing partial β barrel, analogous to the β8 and β12 in UNC5 ZU5 and β8 and β11 in ankyrin-R ZU5 (Figure 5B; Supplementary Figures S4 and S7), and the resulting ZO-1 ZU5/GRINL1A complex assumes a compact, complete ZU5-fold stable in solution. Therefore, the target-binding mode seen in ZO-1 ZU5 can be described as a target-induced domain complementation: the β strands of ZU5 and its target combine to form a complete ZU5-fold.

Importantly, the ZO-1 ZU5-binding sequence of GRINL1A aligns very well, at both amino-acid sequence and secondary structure levels, with a fragment of MRCKβ N-terminal to its C1 domain (Figure 5B). Deletion of parts or the whole of this presumed ZO-1 ZU5-binding sequence disrupted the interaction between MRCKβ and ZO-1 (Figure 5D). Mutations of two hydrophobic residues in either β9 (Phe952 and Tyr954 to

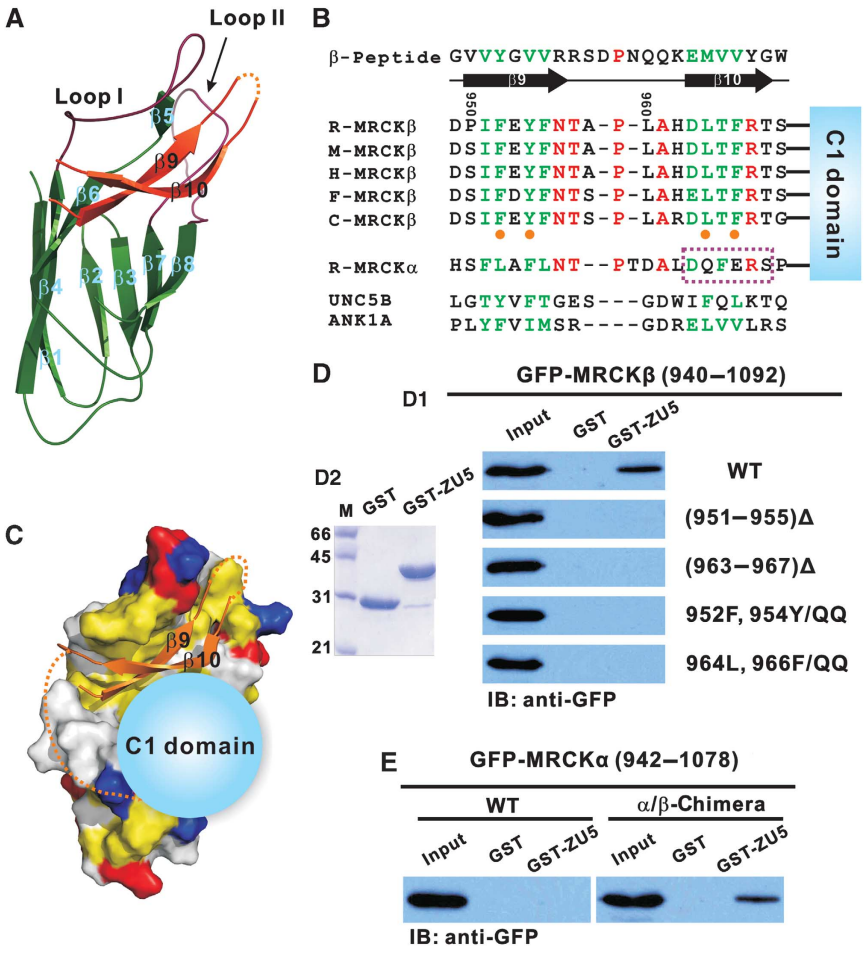


**Figure 5** Structural basis of the ZO-1 ZU5/MRCKβ complex formation. (**A**) Ribbon diagram representation of the ZO-1 ZU5/GRINL1A peptide complex structure. The GRINL1A peptide forms a β-hairpin structure (β9 and β10), and β9 pairs in an anti-parallel manner with two short β strands (β5 and β6) of ZO-1 ZU5. Loop I of the domain becomes structured and interacts with the target peptide. (**B**) Amino-acid sequence alignment of the GRINL1A β-hairpin peptide with the MRCKβ peptide fragment N-terminal to its C1 domain and the equivalent sequences from UNC5B and ankyrin ZU5. Note that the aligned MRCKβ residues corresponding to β9 and β10 of the GRINL1A peptide are highly conserved (in rat, mouse, human, fish, and chicken) and are predicted to form β strands. The residues from MRCKβ are highlighted with orange dots, which are also highly conserved in ZU5 domain from UNC5B and ankyrin, are predicted to be critical for binding to ZO-1 ZU5 based on the ZU5/GRINL1A complex structure, and the roles of these residues in ZO-1 ZU5 binding were directly tested (**D**). In contrast, the corresponding amino acids from MRCKα (the residues aligned to β10 in particular, highlighted by a dashed box in purple) are distinctly different. (**C**) A structural model of the ZO-1 ZU5/MRCKβ ZBD complex. In addition to the N-terminal β-hairpin peptide, the C1 domain of MRCKβ (shown as a blue sphere) is also required for binding to ZO-1 ZU5. (**D**) *In vitro* GST pull-down assay showing the critical roles of the residues forming the predicted β9 and β10 strands of MRCKβ in binding to ZO-1 ZU5. (**E**) The replacement of the MRCKα peptide fragment N-terminal to its C1 domain with the corresponding sequence in MRCKβ converted the MRCKα chimera into a ZO-1 ZU5-binding enzyme. In contrast, the WT MRCKα failed to bind to ZO-1 ZU5.

Gln) or β10 (Leu964 and Phe966 to Gln) also abolished the MRCKβ/ZO-1 complex formation (Figure 5D). It is further noted that the predicted ZO-1 ZU5-binding sequence of MRCKβ is highly conserved among different species (Figure 5B). However, the amino-acid sequence of the corresponding peptide fragment (the predicted β10 sequence in particular) in MRCKα is significantly different from that of MRCKβ (Figure 5B), explaining the observation made earlier that MRCKα does not interact with ZO-1 (Figure 1D). We directly tested the above structure-based analysis by replacing the β10 cassette of MRCKα ('DQFERS') with the corresponding segment from MRCKβ ('DLTFRT'), and found that the resulting MRCKα chimera was capable of binding to ZO-1 (Figure 5E). Taken together, the above structural and biochemical experiments strongly indicate that the peptide fragment preceding the C1 domain of MRCKβ binds to ZO-1 in a β-hairpin conformation, forming a complete ZU5-fold in the ZO-1/MRCKβ complex, although the final proof would have to come from the structure of the ZO-1 ZU5/MRCKβ ZBD complex.

Finally, we note that the structure of the ZO-1 ZU5/GRINL1A peptide complex (and the corresponding MRCKβ β-hairpin peptide complex) still lacks one or two β strands (corresponding to β9 in ankyrin-R ZU5 or β9 and β10 in UNC5 ZU5; Supplementary Figure S7) compared with the complete ZU5-folds. We showed that the C1 domain is also required for binding to ZO-1 ZU5 (Figure 1). It is likely that the MRCKβ C1 domain has an additional structural role in the formation of the MRCKβ/ZO-1 complex (Figure 5C). Supporting this hypothesis, we found that the C1 domain and its preceding β-hairpin sequence together are required for the formation of the stable ZO-1 ZU5/MRCKβ ZBD complex (Supplementary Figure S9). This analysis also provides an explanation for the weak inter-

 

action observed between ZO-1 and the GRINL1A peptide ($K_d \sim 20\,\mu M$) (Supplementary Figure S6D). It is possible that GRINL1A is not a physiological ZO-1 partner, but the protein acted as a useful tool here for us to elucidate the ZO-1 ZU5/MRCKβ interaction mechanism.

### *ZO-1 binds to MRCKβ in a Cdc42-dependent manner*

In our initial attempts to verify the direct binding between ZO-1 ZU5 and the full-length MRCKβ *in vitro*, we failed to detect any interaction (Figure 6A1). A Y2H-based assay also showed that the full-length MRCKβ does not bind to ZO-1 ZU5 (Figure 6A2). We further found that the inclusion of the PH-CH domain tandem C-terminal to the C1 domain sufficiently prevented MRCKβ from binding to ZO-1 ZU5, indicating that the MRCKβ C-terminal tail adopts a closed conformation incapable of binding to ZO-1 (Figure 6A2). The closed conformation of the MRCKβ tail was further confirmed by the observation of a direct interaction between the CC3–C1 domains and the PH-CH-CRIB domains of the enzyme (Supplementary Figure S10A). Interestingly, the removal of the Cdc42-binding CRIB domain did not alter the closed conformation of MRCKβ, implying that the PH-CH domain tandem is largely responsible for the closed conformation of MRCKβ (Figure 6A2).

To investigate the potential opening mechanism of the MRCKβ's closed conformation, we tested the effect of Cdc42 on the binding between MRCKβ and ZO-1 ZU5, as the Cdc42-binding CRIB domain immediately follows the PH-CH tandem. Interestingly, we found that Cdc42-loaded MRCKβ can bind to ZO-1 ZU5, and removal of the CRIB domain abolished the Cdc42-dependent binding of MRCKβ to ZO-1 ZU5 (Figure 6B). Consistent with the above biochemical data, MRCKβ lacking the Cdc42-binding CRIB domain cannot be anchored at the leading edge of migrating COS-7 cells (Figure 6C). Overexpression of a dominant negative form of Cdc42 ('Cdc42N17'; Sudhaharan *et al*, 2009) also eliminated the leading edge localization of MRCKβ (Figure 6D). As a control, MRCKβ was found to localize at the leading edge of cells expressing a constitutively active form of Cdc42 ('Cdc42V12') (Figure 6D). Finally, as phorbol esters are known to bind to the C1 domain of MRCKβ (Choi *et al*, 2008), we tested their potential effects on the opening of the

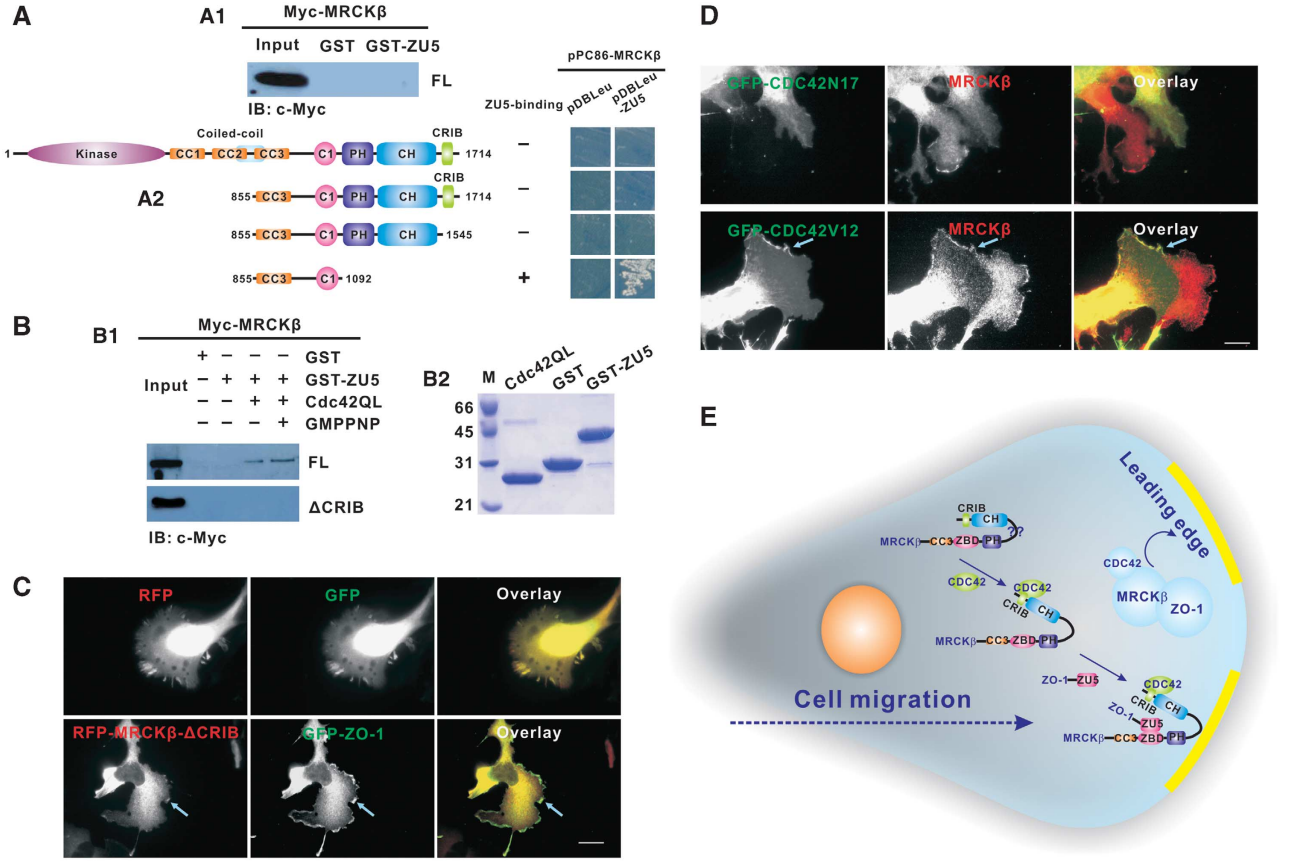


**Figure 6** Cdc42-induced opening of the closed conformation of MRCKβ. (**A**) *In vitro* pull-down experiment showing that the full-length MRCKβ adopts a closed conformation incapable of binding to ZO-1 ZU5 (A1). Y2H-based analysis reveals that the PH-CH tandem is responsible for covering the ZO-1 ZU5-binding site of MRCKβ (A2). (**B**) Binding of active Cdc42 to the CRIB domain releases the closed conformation of MRCKβ, enabling the enzyme to bind to ZO-1. Deletion of the CRIB domain eliminates Cdc42-induced MRCKβ binding to ZO-1. (**C**) The removal of the CRIB domain also dramatically decreases the ZO-1-mediated leading edge localization capacity of MRCKβ. Scale bar: 20 μm. (**D**) The overexpression of a dominant negative form of Cdc42 ('Cdc42N17') resulted in the near complete loss of the leading edge localization of the endogenous MRCKβ. However, overexpression of a constitutive active form of Cdc42 ('Cdc42V12') did not further enhance the leading edge localization of MRCKβ. Scale bar: 20 μm. (**E**) A schematic model showing the Cdc42-dependent binding of MRCKβ to ZO-1. In this model, binding of Cdc42 to the CRIB domain not only activates MRCKβ, but also triggers the activated enzyme to be localized at the leading edge of migrating cells by exposing its ZO-1 ZU5-binding site. The ZO-1-anchored Cdc42/MRCKβ complex at the lamellae is likely to be critical for the directional migration of various types of cells.

MRCKβ's closed conformation. We found that 12-*O*-tetradecanoylphorbol-13-acetate, a commonly used phorbol ester, did not potentiate the MRCKβ/ZO-1 ZU5 complex formation, indicating that phorbol esters cannot by-pass Cdc42 to release the closed conformation of MRCKβ (Supplementary Figure S10B). Taken together, the data shown in Figure 6 uncover that MRCKβ adopts a closed conformation incapable of binding to ZO-1 ZU5. The binding of Cdc42 to its C-terminal CRIB domain induces conformational changes to the neighbouring PH-CH domain tandem, thereby exposing MRCKβ ZBD for binding to ZO-1 (Figure 6E).

### *ZO-1/MRCKβ complex is required for cell migrations*

Finally, we tested the roles of the ZO-1/MRCKβ complex in cell migrations using a wound-healing assay (Figure 7; Rodriguez *et al*, 2005). The control cells showed expected migration-induced wound closure after scratch wounding (Figure 7A). Compared with the scRNA-mediated control (Figure 7B and F), RNAi-mediated knockdown of either ZO-1 or MRCKβ largely eliminated cell movements upon wounding (Figure 7C and G). We checked that the defective cell migrations induced by the ZO-1 or MRCKβ knockdowns are not the results of inhibited cell proliferations (Supplementary Figure S11). Restoring the expression of ZO-1 or MRCKβ effectively rescued cell migration defects induced by RNAi-mediated knockdowns of the two proteins, respectively (Figure 7D and H). In contrast, neither the ZO-1 (ΔZU5) mutant nor the MRCKβ (ΔZBD) mutant rescued cell migration defects induced by the knockdowns (see Figure 7E, I, and J for quantifications), indicating that the direct interaction between ZO-1 and MRCKβ is required for cell migration (with the assumption that these domain deletions specifically disrupt the ZO-1/MRCKβ interaction without other adverse effects). The data in Figure 7, together with the results presented above, demonstrate that ZO-1 has an active role in regulating cell migration by targeting Cdc42-activated MRCKβ at the leading edge of migrating cells.

## Discussion

As a founding member of the MAGUK family of scaffold proteins, ZO-1 is well recognized for its vital roles in the

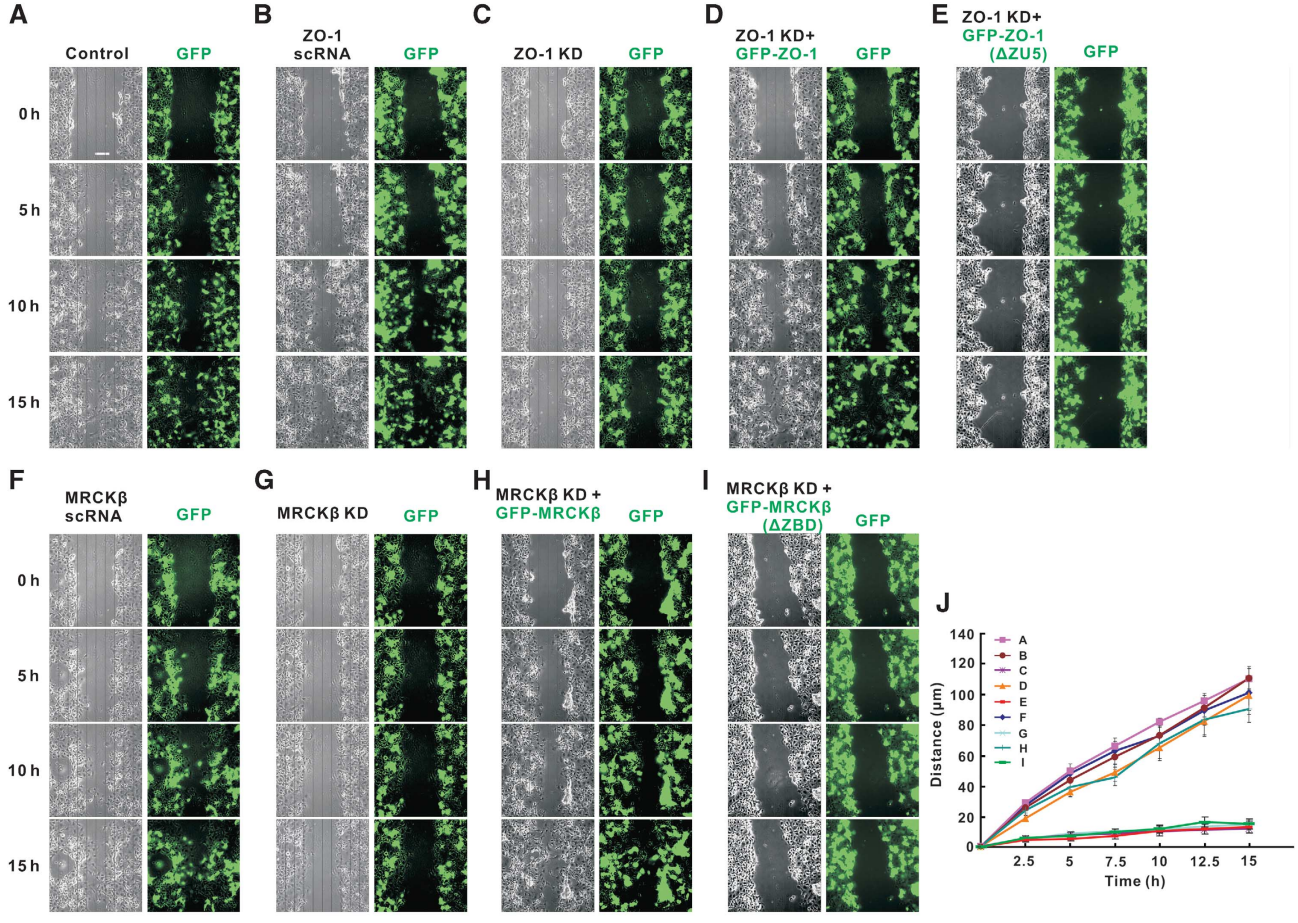


**Figure 7** The ZO-1/MRCKβ complex is essential for cell migration. (**A–I**) Time lapse imaging analysis showing that COS-7 cells display well-characterized, wounding-induced migrations leading to the wound closure. The pSUPER alone and the empty GFP vector were used as the transfection control (**A**). The scRNA of ZO-1 (**B**) and the scRNA of MRCKβ (**F**) had no observable effects on the wound closure (see (**J**) for the quantification). The cell migrations were imaged both with phase contrast mode and with the GFP fluorescence signals. Knockdown of either ZO-1 (**C**) or MRCKβ (**G**) significantly impaired wounding-induced cell migrations. Restored expression of ZO-1 (**D**) or MRCKβ (**H**) rescued cell migration defects induced by the shRNA-mediated knockdowns of the two proteins. In contrast, neither ZO-1 with ZU5 deleted (**E**) nor MRCKβ with ZBD removed (**I**) could rescue cell migration defects. Scale bar: 100 μm. (**J**) Quantification of the imaging experiments are shown in (**A–I**). In this analysis, the migration distances of the cells containing GFP signals were averaged for each condition. Error bars represent s.e.m. from $n = 2$ experiments with 100 cells from each experiment.

assembly of cell–cell adhesion complexes that are critical for the formation of intercellular connection machineries, including TJs and adherens junctions, in a wide variety of tissues (Mitic and Anderson, 1998; Fanning and Anderson, 2009; Tsukita *et al*, 2009). In this work, we show that ZO-1 actively regulates cell migration by binding to the cytoskeletal dynamics regulatory protein kinase MRCKβ, and targeting the enzyme to the leading edge of migrating cells. Our findings reveal that ZO-1, and perhaps other scaffold proteins involved in cell–cell adhesions, can function either as cell-to-cell connectors in maintaining tissue organization or as facilitators in modulating cells migration and tissue remodelling. The ability of ZO-1 to regulate cell migration is highly consistent with the *in vivo* developmental functions of ZO-1 from genetic studies. The severe inhibition of angiogenesis in mice lacking *ZO-1* at early developmental stages could be the result of migration defects of blood vessel endothelial cells (Katsuno *et al*, 2008). The ZO-1/MRCKβ complex in the regulation of cell migration is likely to be important for many human pathological conditions, including cancers. It has been shown that cancer cell migration requires Cdc42-MRCK (Wilkinson *et al*, 2005; Gaggioli *et al*, 2007). Additionally, ZO-1 has been found to be localized at the leading edge of migrating cancer cells together with α5-integrin (Tuomi *et al*, 2009), although it is not clear how the ZO-1/α5-integrin complex promotes cell migration. Our finding of co-localization of ZO-1 and MRCKβ at the leading edge of several migrating human cancer cell lines (Supplementary Figure S2) suggests that the ZO-1/MRCKβ complex might act as downstream of the ZO-1/integrin complex and have a critical role in the cancer cell migration.

The direct interaction between ZO-1 and MRCKβ at the leading edge of migrating cells provides a molecular explanation for ZO-1's role in regulating cell migration and perhaps tissue remodelling. Interestingly, other scaffold proteins have also been implicated to actively participate in the regulation of cell migration, in addition to their well-established roles as scaffolds for cell–cell junction organization. For example, Scribble, another multiple PDZ scaffold protein required for the establishment and maintenance of cell polarity in diverse tissues, has been shown to have active roles in positioning both Cdc42 and PAK in migrating cells (Osmani *et al*, 2006; Nola *et al*, 2008), although Scribble does not directly bind to PAK.

In this work, we also show that MRCKβ adopts a closed conformation incapable of binding to ZO-1 ZU5 (Figure 6). The binding of Cdc42 to the MRCKβ CRIB domain exposes the ZO-1 ZU5-binding site, which is otherwise covered by the PH-CH tandem of the enzyme, even though the CRIB domain is not directly involved in covering the ZO-1 ZU5-binding site (Figure 6E). Thus, ZO-1 specifically binds to the activated form of MRCKβ. It is envisioned that the binding of Cdc42 induces some sort of conformational changes in the PH-CH tandem, thereby allowing the activated MRCKβ to interact with ZO-1. Further work is under progress in elucidating the nature of the Cdc42-induced conformational changes of MRCKβ. In the process of converting cultured cells from confluent states (i.e. with stable cell–cell adhesions) to migrating states, a fraction of ZO-1 moves to the leading edge of cells (Figure 1E), although the molecular basis governing this ZO-1 localization change is unclear at this stage.

ZU5 domain, originally identified as an ~120 amino-acid residue domain present in ZO-1 and UNC5, is also found in various ankyrins and an apoptotic machinery scaffold PIDD (p53-induced protein with a death domain) (Ackerman *et al*, 1997; Leonardo *et al*, 1997; Tinel and Tschopp, 2004; Bennett and Healy, 2008). Although these ZU5 domain-containing proteins are functionally diverse, they are all multi-domain scaffold proteins with no intrinsic enzyme activities. Interestingly, except for ZO-1, which contains an orphan ZU5 domain at its extreme C-terminal end, all other known ZU5 domain proteins contain a UPA domain and a death domain C-terminal to their ZU5 domain (Ipsaro *et al*, 2009). Additionally, ankyrins and PIDD contain two ZU5 domains arranged in tandem. Recently, the structures of the ZU5 domains of UNC5 (Wang *et al*, 2009) and ankyrin-R (Ipsaro *et al*, 2009) have been reported (Supplementary Figure S7). The UNC5 ZU5 domain adopts a β-barrel fold and interacts with its own death domain, and the functions of both the ZU5 and death domains are thereby suppressed by an autoinhibition mechanism (Wang *et al*, 2009). The ankyrin-R ZU5 domain specifically binds to a tandem spectrin repeats (Ipsaro *et al*, 2009). The common theme emerging from these studies, together with this work, is that ZU5 domains function as specific protein–protein interaction modules capable of binding to very different target proteins. A comparison of the structure of ZO-1 ZU5 with those of UNC5 and ankyrin-R ZU5 domains reveals that ZO-1 ZU5 adopts a partial ZU5-fold lacking 2–3 strands at one edge of the β barrel (Supplementary Figure S7). We show here that target proteins bind to ZO-1 ZU5 in a β-sheet conformation. The β strands from the target protein complete the partial ZU5-fold of ZO-1 (i.e. ZO-1 ZU5 binds to its targets via a domain complementation mechanism). The results described in this study not only expand our knowledge of ZU5 domains in general, but also lay a foundation for future investigations of specific cellular functions of ZO-1 that arise from its unique ZU5 domain, which is not present in ZO-2 and ZO-3.

In summary, the identification of the specific interaction between ZO-1 and MRCKβ and the functional characterization of the ZO-1/MRCKβ complex in cell migrations presented in this work uncover a previously uncharacterized role that the classical junctional scaffold protein ZO-1 has in regulating cell migration. The results presented here not only call for further study of this much less explored function of ZO-1 (and perhaps other scaffold proteins involved in cell–cell adhesions) in cell motility, but also indicate to therapeutic possibilities in cancers based on interfering with cancer cell migrations by targeting proteins such as ZO-1.

## Materials and methods

### *Antibodies*

The ZO-1 monoclonal antibody (1A12) and the anti-α-tubulin antibody were purchased from Invitrogen; anti-MRCKα, anti-MRCKβ, and anti-GFP antibodies were purchased from Santa Cruz; and the anti-Myc antibody was purchased from Roche.

### *Protein expression and purification*

DNA sequences encoding human ZO-1 ZU5 domain (residues 1631–1748), various mutants, the fused ZO-1 ZU5/GRINL1A complex, and Cdc42QL were individually cloned into a modified version of the pET32a vector. The resulting ZU5 domain constructs, the fused

ZO-1 ZU5/GRINL1A complex, and Cdc42QL each contained a $His_6$-tag in the N-terminus. Point mutations of ZU5 proteins were created using the standard PCR-based mutagenesis method and confirmed by DNA sequencing. Recombinant proteins were expressed in *Escherichia coli* BL21 (DE3) host cells at 16°C. $His_6$-tagged ZU5 proteins and the fused ZO-1 ZU5/GRINL1A complex expressed in bacterial cells were purified by $Ni^{2+}$-NTA agarose (Qiagen) affinity chromatography followed by size-exclusion chromatography. Uniformly, $^{15}N$ or $^{15}N$, $^{13}C$-labelled ZU5 proteins and the fused ZO-1 ZU5/GRINL1A complex were prepared by growing bacteria in M9 minimal medium using $^{15}NH_4Cl$ as the sole nitrogen source or $^{15}NH_4Cl$ and $^{13}C_6$-glucose (Cambridge Isotope Laboratories Inc.) as the sole nitrogen and carbon sources, respectively.

### *NMR structure determination*

NMR samples contained 1.0 mM of the ZU5 protein and the fused ZO-1 ZU5/GRINL1A complex in 50 mM Tris (pH 7.0, with 1 mM DTT, and 1 mM EDTA) in 90% $H_2O$/10% $D_2O$ or 99.9% $D_2O$. NMR spectra were acquired at 35°C on Varian Inova 500 or 750 MHz spectrometers. Backbone and side-chain resonance assignments of ZU5 proteins were achieved by the standard heteronuclear correlation experiments (Bax and Grzesiek, 1993; Kay and Gardner, 1997). The side chains of aromatics were assigned using $^1H$ two-dimensional total correlation spectroscopy/NOESY experiments. Approximate inter-proton distance restraints were derived from NOESY experiments (a $^1H$ 2D homonuclear NOESY, a $^{15}N$-separated NOESY, and a $^{13}C$-separated NOESY). Structures were calculated using the program CNS (Brunger *et al*, 1998).

### *Yeast two-hybrid screening*

Y2H was performed using the WT ZO-1 ZU5 domain as the bait. Human ZO-1 (residues 1631–1748) was subcloned into the pDBLeu vector. The bait plasmid and a random-primed cDNA library from rat hippocampus in pPC86 vector were transformed into PJ69-4A yeast cells and grown on quadruple minus plates that lack leucine, tryptophan, adenine, and histidine. Positive clones were scored by both growth and blue assays (Cao *et al*, 2007). Plasmid cDNAs from positive clones were recovered and back-transformed with either the bait or the empty pDBLeu vector into both PJ69-4A and HF7c yeast strains to confirm the interaction. All of the cDNA constructs were confirmed by sequencing.

### *GST pull-down assays*

Crude extracts of various fragments of N-terminal Myc- or GFP-tagged MRCKβ expressed in HEK293 cells were first incubated with 50 μl of Glutathione Sepharose™ 4B Fast Flow (GE Healthcare) 50% slurry beads in a lysis buffer (50 mM HEPES, pH 7.6, 150 mM NaCl, 1.5 mM $MgCl_2$, 100 mM NaF, 1 mM EGTA, 1% Triton, 10% glycerol, and various protease inhibitors) for half an hour. The cleared supernatants were transferred to a new batch of 50 μl slurry beads, mixed with GST or GST-tagged proteins (10 μl from 1 mg/ml stock solutions) for 2 h at 4°C. After washing the beads three times with the lysis buffer, the proteins captured by the beads were eluted by boiling with the SDS–PAGE sample buffer, resolved by SDS–PAGE, and detected either by Coomassie blue staining or by immunoblotting with specific antibodies. Purified His-tagged Cdc42QL was incubated with 100 μM GTP analogue GMPPNP in a reaction buffer (50 mM Tris, 200 mM $(NH_4)_2SO_4$, pH 8.5) for 5 h before mixing with GST-tagged proteins.

### *Co-immunoprecipitations*

For immunoprecipitation of overexpressed proteins, COS-7 cells grown on 100 mm culture dishes were co-transfected with specific cDNA constructs. Cells were harvested 4 h after wounding. Each cell lysate was incubated with 50 μl protein G beads (50% slurry) in the lysis buffer for 1 h, and transferred to a tube containing 50 μl protein G beads (50% slurry) and 2.5 μg anti-ZO-1 antibody. After incubation for 4 h at 4°C, the beads were washed with the lysis buffer three times. The captured proteins were then eluted using the SDS–PAGE buffer and analysed with specific antibodies.

### *Cell culture, immunostaining, and imaging*

All cDNA constructs used in this study were cloned into mammalian expression vector pEGFP (Invitrogen) and pERFP for imaging studies, and pCMV-Myc (Invitrogen) and pEGFP (Invitrogen) for pull-down assays. The pSUPER vector was used to drive the expression of shRNA in COS-7 cells. The shRNAs used in this study include ZO-1 (KD1: GATCAAATTCTCAGGGTAA; KD2: CCGAA GAAGTTTTGAGAAT), and MRCKβ (KD1: CCGAAGAGCTCGAGG CTTT; KD2: TCGAGAAGACTTTGAAATA; KD3: GATAAATACGAAC GAGAAA). The scramble siRNAs were designed using siRNA Wizard™ v3.1. COS-7 cells and HEK293 cells were cultured in minimum essential medium supplemented with 10% fetal bovine serum (FBS). Transfection of HEK293 cells with plasmid DNA was performed using Lipofectamine (Invitrogen) according to the manufacturer's instructions. Transfection of COS-7 cells with plasmid DNA, shRNA or scRNA was performed by electroporation (Amaxa Biosystems). In the knockdown experiments, cells were fixed ~50 h after transfection. In immunofluorescence studies, cells on cover slips were fixed with 4% paraformaldehyde for 20 min. Cells expressing the transfected constructs were identified by immumostaining of the N-terminal tag with corresponding primary and secondary antibodies. For the immunostaining of endogenous proteins, cells were incubated with primary antibody at 4°C overnight. Alexa 488- and Alexa 594-conjugated secondary antibodies against goat and mouse immunoglobulin were obtained from Molecular Probes. All images were acquired on a Nikon TE2000E inverted fluorescent microscope.

### *Wound-healing assays and cell proliferation analysis*

COS-7 cells at about 90% confluence were scratched with a pipette tip and replaced in fresh 10% FBS-containing medium to induce cell migrations. Images were processed with the MetaMorph software package. Cell proliferations of COS-7 cells used for the wound-healing assays were measured with WST-1 (Dojindo) according to the manufacturer's protocol.

### *Illustrations*

The protein structure figures were prepared using the programs MOLMOL (Koradi *et al*, 1996) and PyMOL (http://pymol.sourceforge.net/).

### *Coordinates*

The atomic coordinates of ZO-1 ZU5_MC/AA mutant and ZO-1 ZU5/GRINL1A complex have been deposited in the Protein Data Bank with accession codes 2KXR and 2KXS, respectively.

### *Supplementary data*

Supplementary data are available at *The EMBO Journal* Online (http://www.embojournal.org).

## Acknowledgements

We thank Dr Thomas Leung for MRCKβ cDNA, Drs Alan Fanning and Ian Macara for providing the human ZO-1 cDNA, Dr Raymond Roginski for the GRINL1A cDNA, Miss Ling-Nga Chan and Jia Chen for technical assists, and Mr Anthony Zhang for editing of the manuscript. This work was supported by grants from the Research Grants Council of Hong Kong to MZ (HKUST663407, 663808, 664009, CA07/08.SC01, SEG_HKUST06, and AoE/B-15/01-II), WF (660708 and 660709), and JX (HKUST6/CRF/08 and 663107), the National Major Basic Research Program of China (2009CB918600 and 2011CB910500), the National Natural Science Foundation of China (31070657), and the Knowledge Innovation Program of the Chinese Academy of Sciences (KSCX2-YW-R-154).

*Author contributions*: LH, WF, WW, RW, and MZ designed the experiments; LH, WW, and RW performed all of the experiments except the initial Y2H screening; CK and JX performed the initial Y2H screening, LH, WW, RW, WF, and MZ analysed the data; LH, WF, and MZ wrote the paper; and MZ coordinated the entire research project.

## Conflict of interest

The authors declare that they have no conflict of interest.

 

## References

Ackerman SL, Kozak LP, Przyborski SA, Rund LA, Boyer BB, Knowles BB (1997) The mouse rostral cerebellar malformation gene encodes an UNC-5-like protein. *Nature* **386:** 838–842

Anderson JM, Fanning AS, Lapierre L, Van Itallie CM (1995) Zonula occludens (ZO)-1 and ZO-2: membrane-associated guanylate kinase homologues (MAGuKs) of the tight junction. *Biochem Soc Trans* **23:** 470–475

Anderson JM, Van Itallie CM, Fanning AS (2004) Setting up a selective barrier at the apical junction complex. *Curr Opin Cell Biol* **16:** 140–145

Balda MS, Matter K (1998) Tight junctions. *J Cell Sci* **111** (Part 5)**:** 541–547

Bax A, Grzesiek S (1993) Methodological advaces in protein NMR. *Acc Chem Res* **26:** 131–138

Bennett V, Healy J (2008) Organizing the fluid membrane bilayer: diseases linked to spectrin and ankyrin. *Trends Mol Med* **14:** 28–36

Brunger AT, Adams PD, Clore GM, DeLano WL, Gros P, Grosse-Kunstleve RW, Jiang JS, Kuszewski J, Nilges M, Pannu NS, Read RJ, Rice LM, Simonson T, Warren GL (1998) Crystallography & NMR system: a new software suite for macromolecular structure determination. *Acta Crystallogr D Biol Crystallogr* **54** (Part 5)**:** 905–921

Cao M, Xu J, Shen C, Kam C, Huganir RL, Xia J (2007) PICK1-ICA69 heteromeric BAR domain complex regulates synaptic targeting and surface expression of AMPA receptors. *J Neurosci* **27:** 12945–12956

Choi SH, Czifra G, Kedei N, Lewin NE, Lazar J, Pu Y, Marquez VE, Blumberg PM (2008) Characterization of the interaction of phorbol esters with the C1 domain of MRCK (myotonic dystrophy kinase-related Cdc42 binding kinase) alpha/beta. *J Biol Chem* **283:** 10543–10549

Citi S, Sabanay H, Jakes R, Geiger B, Kendrick-Jones J (1988) Cingulin, a new peripheral component of tight junctions. *Nature* **333:** 272–276

D'Atri F, Citi S (2002) Molecular complexity of vertebrate tight junctions (Review). *Mol Membr Biol* **19:** 103–112

Fanning AS, Anderson JM (2009) Zonula occludens-1 and -2 are cytosolic scaffolds that regulate the assembly of cellular junctions. *Ann NY Acad Sci* **1165:** 113–120

Fanning AS, Jameson BJ, Jesaitis LA, Anderson JM (1998) The tight junction protein ZO-1 establishes a link between the transmembrane protein occludin and the actin cytoskeleton. *J Biol Chem* **273:** 29745–29753

Furuse M, Fujita K, Hiiragi T, Fujimoto K, Tsukita S (1998) Claudin-1 and -2: novel integral membrane proteins localizing at tight junctions with no sequence similarity to occludin. *J Cell Biol* **141:** 1539–1550

Furuse M, Hirase T, Itoh M, Nagafuchi A, Yonemura S, Tsukita S (1993) Occludin: a novel integral membrane protein localizing at tight junctions. *J Cell Biol* **123:** 1777–1788

Gaggioli C, Hooper S, Hidalgo-Carcedo C, Grosse R, Marshall JF, Harrington K, Sahai E (2007) Fibroblast-led collective invasion of carcinoma cells with differing roles for RhoGTPases in leading and following cells. *Nat Cell Biol* **9:** 1392–1400

Goh KL, Yang JT, Hynes RO (1997) Mesodermal defects and cranial neural crest apoptosis in alpha5 integrin-null embryos. *Development* **124:** 4309–4319

Gomes ER, Jani S, Gundersen GG (2005) Nuclear movement regulated by Cdc42, MRCK, myosin, and actin flow establishes MTOC polarization in migrating cells. *Cell* **121:** 451–463

Gonzalez-Mariscal L, Betanzos A, Avila-Flores A (2000) MAGUK proteins: structure and role in the tight junction. *Semin Cell Dev Biol* **11:** 315–324

Gonzalez-Mariscal L, Betanzos A, Nava P, Jaramillo BE (2003) Tight junction proteins. *Prog Biophys Mol Biol* **81:** 1–44

Gonzalez-Mariscal L, Islas S, Contreras RG, Garcia-Villegas MR, Betanzos A, Vega J, Diaz-Quinonez A, Martin-Orozco N, Ortiz-Navarrete V, Cereijido M, Valdes J (1999) Molecular characterization of the tight junction protein ZO-1 in MDCK cells. *Exp Cell Res* **248:** 97–109

Haskins J, Gu L, Wittchen ES, Hibbard J, Stevenson BR (1998) ZO-3, a novel member of the MAGUK protein family found at the tight junction, interacts with ZO-1 and occludin. *J Cell Biol* **141:** 199–208

Hurd TW, Gao L, Roh MH, Macara IG, Margolis B (2003) Direct interaction of two polarity complexes implicated in epithelial tight junction assembly. *Nat Cell Biol* **5:** 137–142

Ide N, Hata Y, Nishioka H, Hirao K, Yao I, Deguchi M, Mizoguchi A, Nishimori H, Tokino T, Nakamura Y, Takai Y (1999) Localization of membrane-associated guanylate kinase (MAGI)-1/BAI-associated protein (BAP) 1 at tight junctions of epithelial cells. *Oncogene* **18:** 7810–7815

Ipsaro JJ, Huang L, Mondragon A (2009) Structures of the spectrin-ankyrin interaction binding domains. *Blood* **113:** 5385–5393

Itoh M, Furuse M, Morita K, Kubota K, Saitou M, Tsukita S (1999) Direct binding of three tight junction-associated MAGUKs, ZO-1, ZO-2, and ZO-3, with the COOH termini of claudins. *J Cell Biol* **147:** 1351–1363

Itoh M, Nagafuchi A, Moroi S, Tsukita S (1997) Involvement of ZO-1 in cadherin-based cell adhesion through its direct binding to alpha catenin and actin filaments. *J Cell Biol* **138:** 181–192

Itoh M, Nagafuchi A, Yonemura S, Kitani-Yasuda T, Tsukita S (1993) The 220-kD protein colocalizing with cadherins in non-epithelial cells is identical to ZO-1, a tight junction-associated protein in epithelial cells: cDNA cloning and immunoelectron microscopy. *J Cell Biol* **121:** 491–502

Jesaitis LA, Goodenough DA (1994) Molecular characterization and tissue distribution of ZO-2, a tight junction protein homologous to ZO-1 and the Drosophila discs-large tumor suppressor protein. *J Cell Biol* **124:** 949–961

Katsuno T, Umeda K, Matsui T, Hata M, Tamura A, Itoh M, Takeuchi K, Fujimori T, Nabeshima Y, Noda T, Tsukita S (2008) Deficiency of zonula occludens-1 causes embryonic lethal phenotype associated with defected yolk sac angiogenesis and apoptosis of embryonic cells. *Mol Biol Cell* **19:** 2465–2475

Kay LE, Gardner KH (1997) Solution NMR spectroscopy beyond 25 kDa. *Curr Opin Struct Biol* **7:** 722–731

Kim SK (1995) Tight junctions, membrane-associated guanylate kinases and cell signaling. *Curr Opin Cell Biol* **7:** 641–649

Koradi R, Billeter M, Wuthrich K (1996) MOLMOL: a program for display and analysis of macromolecular structures. *J Mol Graph* **14:** 51–55, 29–32

Leonardo ED, Hinck L, Masu M, Keino-Masu K, Ackerman SL, Tessier-Lavigne M (1997) Vertebrate homologues of C. elegans UNC-5 are candidate netrin receptors. *Nature* **386:** 833–838

Leung T, Chen XQ, Tan I, Manser E, Lim L (1998) Myotonic dystrophy kinase-related Cdc42-binding kinase acts as a Cdc42 effector in promoting cytoskeletal reorganization. *Mol Cell Biol* **18:** 130–140

Martin-Padura I, Lostaglio S, Schneemann M, Williams L, Romano M, Fruscella P, Panzeri C, Stoppacciaro A, Ruco L, Villa A, Simmons D, Dejana E (1998) Junctional adhesion molecule, a novel member of the immunoglobulin superfamily that distributes at intercellular junctions and modulates monocyte transmigration. *J Cell Biol* **142:** 117–127

Matter K, Balda MS (2003) Functional analysis of tight junctions. *Methods* **30:** 228–234

McNeil E, Capaldo CT, Macara IG (2006) Zonula occludens-1 function in the assembly of tight junctions in Madin-Darby canine kidney epithelial cells. *Mol Biol Cell* **17:** 1922–1932

Mitic LL, Anderson JM (1998) Molecular architecture of tight junctions. *Annu Rev Physiol* **60:** 121–142

Nola S, Sebbagh M, Marchetto S, Osmani N, Nourry C, Audebert S, Navarro C, Rachel R, Montcouquiol M, Sans N, Etienne-Manneville S, Borg JP, Santoni MJ (2008) Scrib regulates PAK activity during the cell migration process. *Hum Mol Genet* **17:** 3552–3565

Osmani N, Vitale N, Borg JP, Etienne-Manneville S (2006) Scrib controls Cdc42 localization and activity to promote cell polarization during astrocyte migration. *Curr Biol* **16:** 2395–2405

Rodriguez LG, Wu X, Guan JL (2005) Wound-healing assay. *Methods Mol Biol* **294:** 23–29

Roginski RS, Mohan Raj BK, Birditt B, Rowen L (2004) The human GRINL1A gene defines a complex transcription unit, an unusual form of gene organization in eukaryotes. *Genomics* **84:** 265–276

Roh MH, Makarova O, Liu CJ, Shin K, Lee S, Laurinec S, Goyal M, Wiggins R, Margolis B (2002) The Maguk protein, Pals1, functions as an adapter, linking mammalian homologues of Crumbs and Discs Lost. *J Cell Biol* **157:** 161–172

Ryeom SW, Paul D, Goodenough DA (2000) Truncation mutants of the tight junction protein ZO-1 disrupt corneal epithelial cell morphology. *Mol Biol Cell* **11:** 1687–1696

Schneeberger EE, Lynch RD (2004) The tight junction: a multifunctional complex. *Am J Physiol Cell Physiol* **286:** C1213–C1228

Stevenson BR, Siliciano JD, Mooseker MS, Goodenough DA (1986) Identification of ZO-1: a high molecular weight polypeptide associated with the tight junction (zonula occludens) in a variety of epithelia. *J Cell Biol* **103:** 755–766

Sudhaharan T, Liu P, Foo YH, Bu W, Lim KB, Wohland T, Ahmed S (2009) Determination of *in vivo* dissociation constant, KD, of Cdc42-effector complexes in live mammalian cells using single wavelength fluorescence cross-correlation spectroscopy. *J Biol Chem* **284:** 13602–13609

Tan I, Yong J, Dong JM, Lim L, Leung T (2008) A tripartite complex containing MRCK modulates lamellar actomyosin retrograde flow. *Cell* **135:** 123–136

Tinel A, Tschopp J (2004) The PIDDosome, a protein complex implicated in activation of caspase-2 in response to genotoxic stress. *Science* **304:** 843–846

Tsukita S, Katsuno T, Yamazaki Y, Umeda K, Tamura A (2009) Roles of ZO-1 and ZO-2 in establishment of the belt-like adherens and tight junctions with paracellular permselective barrier function. *Ann NY Acad Sci* **1165:** 44–52

Tuomi S, Mai A, Nevo J, Laine JO, Vilkki V, Ohman TJ, Gahmberg CG, Parker PJ, Ivaska J (2009) PKCepsilon regulation of an alpha5 integrin-ZO-1 complex controls lamellae formation in migrating cancer cells. *Sci Signal* **2:** ra32

Umeda K, Ikenouchi J, Katahira-Tayama S, Furuse K, Sasaki H, Nakayama M, Matsui T, Tsukita S, Furuse M (2006) ZO-1 and ZO-2 independently determine where claudins are polymerized in tight-junction strand formation. *Cell* **126:** 741–754

Wang R, Wei Z, Jin H, Wu H, Yu C, Wen W, Chan LN, Wen Z, Zhang M (2009) Autoinhibition of UNC5b revealed by the cytoplasmic domain structure of the receptor. *Mol Cell* **33:** 692–703

Wilkinson S, Paterson HF, Marshall CJ (2005) Cdc42-MRCK and Rho-ROCK signalling cooperate in myosin phosphorylation and cell invasion. *Nat Cell Biol* **7:** 255–261

Willott E, Balda MS, Fanning AS, Jameson B, Van Itallie C, Anderson JM (1993) The tight junction protein ZO-1 is homologous to the Drosophila discs-large tumor suppressor protein of septate junctions. *Proc Natl Acad Sci USA* **90:** 7834–7838

Woods DF, Bryant PJ (1993) ZO-1, DlgA and PSD-95/SAP90: homologous proteins in tight, septate and synaptic cell junctions. *Mech Dev* **44:** 85–89

Xu J, Kausalya PJ, Phua DC, Ali SM, Hossain Z, Hunziker W (2008) Early embryonic lethality of mice lacking ZO-2, but not ZO-3, reveals critical and nonredundant roles for individual zonula occludens proteins in mammalian development. *Mol Cell Biol* **28:** 1669–1678

 